

The Influence of Synthesis Conditions on Hydroxyapatite Adsorption Characteristics in the Process of Zn(II) and Pb(II) Removal from Single and Binary Solutions

RODICA ELENA PATESCU¹, CLAUDIA MARIA SIMONESCU¹, GHEORGHE NECHIFOR^{*, 2}, CHRISTU TARDEF², IONELA CAMELIA IONASCU¹

¹ University Politehnica of Bucharest, Faculty of Applied Chemistry and Materials Science, 1-7 Polizu Str., 011061, Bucharest, Romania,

² National Institute for R&D in Electrical Engineering ICPE-CA, 313 Splaiul Unirii, 030138, Bucharest, Romania

Two types of nanohydroxyapatite samples have been obtained by wet chemical precipitation synthesis, involving calcium nitrate tetrahydrate and diammonium hydrogen phosphate as precursors in different conditions. Powders obtained were characterized by X-ray diffraction (XRD) and FTIR spectroscopy. The equilibrium isotherm models related with lead and zinc ions removal from synthetic aqueous solutions have been also investigated. According to this research study, it has been found that the nanohydroxyapatite samples show good heavy metals adsorption capacity, and selectivity for lead ions. It was also observed a slow decreasing of sorption capacity of heavy metal ions from binary solutions compared to that registered from single heavy metal ion solutions.

Keywords: synthetic nanohydroxyapatite, wet chemical precipitation, sorption capacity, lead and zinc removal

Anthropogenic activities, especially industrial ones, have significant negative effects on the environment and on health. These negative effects are due to the main pollutants that wastes (solid, liquid and gaseous) can contain. Among the main pollutants of the environment, heavy metals and polycyclic aromatic hydrocarbons are included in the category of toxic pollutants. As a result, the need to remove and/or to recover these pollutants from the waste/wastewater they contain is becoming more and more evident. With regard to heavy metals, the most efficient and cost-effective disposal method is adsorption. Numerous research studies have been carried out in recent years on the removal of heavy metals from synthetic solutions and wastewaters through sorption processes [1-5]. This is mainly due to the advantages of design flexibility, reduced costs, ease of handling and operation, the possibility of using as an adsorbent a very large number of materials (natural, synthetic and even wastes), the obtaining of high quality effluents and the possibility of regeneration and reuse of adsorbents [6].

The most common adsorbents are activated carbon [7], zeolites [8], clays [9], biomass [10] and polymeric materials [11]. Some of these adsorbents are characterized by reduced sorption capacity, but also inconveniences due to their separation. As a result, there is a need to develop new adsorbents with improved surface characteristics and performance in terms of selectivity and sorption capacity.

A safe method to inactivate heavy metals is to bind them in the form of insoluble salts which can not be washed by water. For this reason, it is proposed to use the hydroxyapatite, $\text{Ca}_{10}(\text{PO}_4)_6(\text{OH})_2$ (HAP), obtained by a traditional method of wet precipitation under different synthesis conditions. The motivation for choosing of this ceramic compound lies in its high ability to immobilize contaminants, high oxidation/reducing stability, and reduced water solubility. Also it is known that the crystal structure $(\text{A}_4^{\text{I}})(\text{A}_6^{\text{II}})(\text{BO}_4)_6(\text{X}_2)$ of HAP allows a high degree

of disorder structural due to multiple chemicals substitutions.

Numerous studies have highlighted that the reactivity and ability to retain heavy metals is very closely related to the particularities (composition, particle's size, morphology) of the adsorbent material, mainly the electrical charge of the surface, the size and specific surface area thereof [12-16].

As a result, one of the main objectives of this research study is to establish the effect of process variables (pH, maturation time, synthesis temperature) on the specific surface area, morphology, degree of crystallinity and capacity of lead and zinc ions removal from aqueous solutions. One other objective is to evaluate the sorption capacity of nanohydroxyapatite powders obtained in batch experiments with single and binary lead and zinc ions solutions. Kinetic and equilibrium studies have been also performed to state the kinetic model and the equilibrium isotherm that characterize the sorption process.

Experimental part

Materials

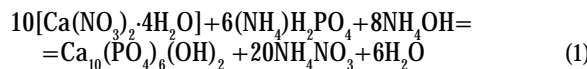
Calcium nitrate tetrahydrate ($\text{Ca}(\text{NO}_3)_2 \cdot 4\text{H}_2\text{O}$), diammonium hydrogen phosphate ($(\text{NH}_4)_2\text{HPO}_4$) and ammonium hydroxide (NH_4OH) are of analytical grade being purchased from Merck, Germany. Stock solutions of 1000 mg Pb(II)/L and 1000 mg Zn(II)/L were prepared from lead nitrate (Merck, Germany) and zinc nitrate (Merck, Germany). These stock solutions were diluted to prepare single and binary heavy metals solution with desired concentrations. Nitric acid HNO_3 65% Suprapur® Sigma-Aldrich and NH_4OH from Merck, Germany were used to modify the solution's pH without further purification.

Synthesis of hydroxyapatite samples

A wet synthesis method was used to obtain HAP nanoparticles. This involves pH higher than 9 (to ensure the apatite structure formation) and reaction temperature

* email: doru.nechifor@yahoo.com

between 40 and 90°C. Higher temperatures favor the formation of compounds with high degree of crystallinity. Precipitation method used involves precursors such as $\text{Ca}(\text{NO}_3)_2 \cdot 4\text{H}_2\text{O}$ and $(\text{NH}_4)_2\text{HPO}_4$ (Merck KGaA, Germany) at a stoichiometry corresponding to $\text{Ca}_{10}(\text{PO}_4)_6(\text{OH})_2$ for which the ratio Ca/P is 1.67. Preparation of hydroxyapatite was carried out under specified conditions of temperature and pH, according to the overall reaction presented below:



The solutions of $\text{Ca}(\text{NO}_3)_2$ and $(\text{NH}_4)_2\text{HPO}_4$ were separately prepared and stirred for 30 min. Then, $(\text{NH}_4)_2\text{HPO}_4$ solution was slowly added to the $\text{Ca}(\text{NO}_3)_2 \cdot 4\text{H}_2\text{O}$ solution and pH was increased to 9 using NH_4OH . The reaction was performed at 80°C for 120 min and stirred intensively. During the reaction, the pH was controlled in order to keep it above 9. Then the suspension was kept under the mother liquid conditions for 2 h at room temperature for aging. The precipitate was filtered through Whatman 41 filter paper, washed three times with doubly distilled water. Then the precipitates were washed with distilled water several times to remove nitrate and ammonium ions, dried at 90 °C for 16 h (HAP-1 sample).

Biphase calcium phosphate with the higher amount of hydroxyapatite ($\text{Ca}_{10}(\text{PO}_4)_6(\text{OH})_2$) with (β -tricalcium phosphate (β -TCP)) was prepared by solution route using the analytical reagent grade calcium nitrate tetrahydrate $[\text{Ca}(\text{NO}_3)_2 \cdot 4\text{H}_2\text{O}]$ and di-ammonium hydrogen orthophosphate $[(\text{NH}_4)_2\text{HPO}_4]$. HAP was precipitated at room temperature in aqueous medium by the slow addition of diammonium hydrogen orthophosphate containing NH_4OH solution (for maintaining pH~10) to a solution of calcium nitrate tetrahydrate (also containing NH_4OH solution for maintaining pH~10). The solution was stirred constantly for 2h by a mechanical stirrer, allowing the reaction to complete. The resultant precipitate was filtered and dried. Aggregates formed were crushed to get fine powder after which was calcined at 900°C. This sample has been noted as HAP-2.

Characterization of hydroxyapatite samples

After synthesis, the adsorbents have been characterized by the use of X-ray diffraction (XRD). Phase composition and crystallinity and phase composition of hydroxyapatite samples prepared were determined by X-ray diffraction (XRD, Bruker D8Discover, Germany) with $\text{CuK}\alpha$ radiation at $\lambda = 1.5406 \text{ \AA}$. X-ray diffractograms were registered at

2θ range of 10-60° and step size of 0.04° at a count time of 1 s.

The presence of functional groups was analyzed by FTIR spectroscopy using a SHIMADZU 8400 Spectrometer in the 400-4000 cm^{-1} range.

The N_2 adsorption/desorption isotherms for BET specific surface area measurements were recorded on a Micromeritics ASAP 2020 analyzer. Before analysis both samples were outgassed at 120°C for at least 6 h under vacuum.

Sorption studies

Sorption batch experiments were carried out at room temperature in duplicate to determine the sorption capacity of sorbents tested. Three sets of experiments were performed.

Both heavy metal ions concentration in the initial solutions and after the sorption experiments has been determined by atomic absorption spectrometry on a Contra®300 AAS Atomic Adsorption Spectrometer. All the sorption experiments have been performed on a GFL Shaker 3015 at 150 rpm.

The concentration of heavy metals in all the experimental sets is introduced in table 1.

To reveal the effect of the solution's pH on the adsorption process, the experiments were carried out at the following operating conditions: 50 mL heavy metal ions solution, 50 mg of nano-HAP, room temperature, 150 rpm speed rotation, for 24 h and pH range of 1.6 -6.5 for lead ions and 1.6-8.25 for zinc ions solution.

To determine the effect of the time, the experiments were performed at the same conditions as those for the pH's effect, at the optimum pH previously determined, and the time varied from 5 to 420 min.

The sorption isotherm has been set from experiments at equilibrium with the pollutant's solutions at concentrations presented in table 1. After each experiment, the solution was filtered and the filtrate was analyzed by AAS to determine the residual level of each pollutant in solution.

The sorption capacity and the amount of both heavy metal ions adsorbed by nano-HAP particles (mg/g) were calculated with the following equation:

$$Q = \frac{(C_i - C_e) \times V}{m} \quad (2)$$

where Q designates heavy metal ions uptake (mg/g), C_i represents the pollutant's concentration in the initial solution (mg/L), C_e is the pollutant's concentration in the

Concentration of Pb(II) in the single solution (mg/L)	Concentration of Zn(II) in the single solution (mg/L)	Binary solutions	
		Pb(II) (mg/L)	Zn(II) (mg/L)
107	100.82	100.53	94.7
75.81	76.23	76.17	74.33
50.31	50.22	58.48	50.36
25.03	25.09	39.24	40.5
13.39	12.97	29.16	26.53
4.26	5.03	14.77	15.21
		5.8	6.45

Table 1
THE SINGLE AND BINARY
SOLUTIONS USED IN THE
EXPERIMENTS

solution at equilibrium (mg/L), V – solution's volume (L), and m - mass of nano-HAP used (g).

Results and discussions

Characterization of hydroxyapatite samples

The two samples of hydroxyapatite have been characterized by using X-ray Diffraction. X-ray patterns of HAP samples are illustrated in figure 1.

The crystalline phases were determined from a comparison of the registered standard JCPDS (Joint Committee on Powder Diffraction File) database (HAP: 09-0432, β -TCP: 09-0169) with the obtained powder diffraction files. The intensity ratio between HAP and TCP in all synthesized powder was determined using the relative intensity ratio (RIR) method [17].

As it can be seen from figure 1, in the case of sample dried at 90°C for 16 h (HAP-1 sample), all the diffraction peaks can be indexed as hydroxyapatite indicating that HAP is the single phase obtained. The characteristic peaks of HAP appears in figure 1 at $2\theta \approx 25.9^\circ, 31.8^\circ, 32.8^\circ, 34.1^\circ, 43.7^\circ$, and 49.4° [18].

However, in case of calcined sample, the diffraction peaks can be indexed as hydroxyapatite and tricalcium phopshate (β -TCP). No other crystalline impurity was detected. Thus, calcination leads to obtain a mixture formed by hydroxyapatite and β -TCP.

The sharp peaks of the diffractograms for HAP samples illustrate that both materials are crystalline powders. However, the sharpness of the diffraction peaks increases with increasing sintering temperature. As such, the broadest diffraction peaks are observed for samples synthesized at the lowest studied temperature (100°C), whilst the narrowest diffraction peaks are observed for those synthesized at the highest studied temperature (900°C). Increase in sharpness of the XRD peaks represents the increase in the crystallinity of the HAP powders.

The average grain size of the HAP powders was estimated from X-ray diffraction data, on the 0 0 2 peak, using Scherrer equation (3):

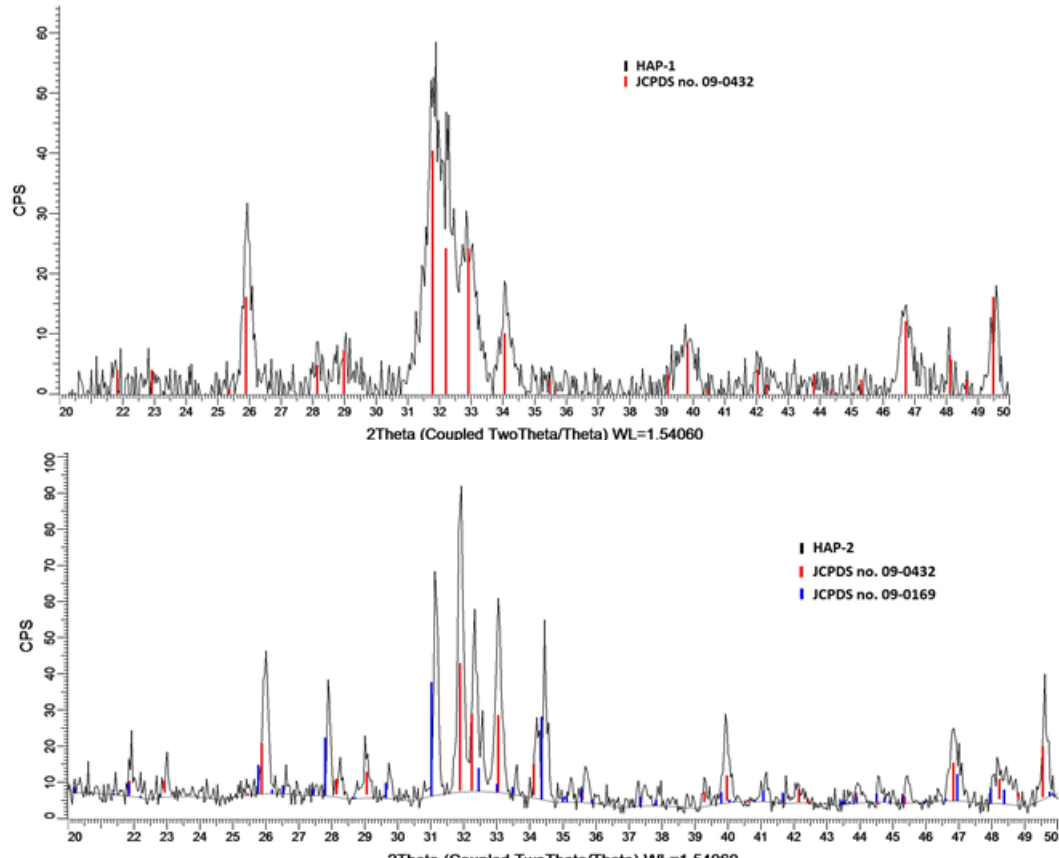


Fig. 1. XRD patterns of HAP samples

$$D_{hkl} = \frac{k\lambda}{FWHM \cos \theta} \quad (3)$$

where, k is the shape factor equal to 0.9, λ the X-ray wavelength (equal to 1.541 Å for Cu K radiation), θ the Bragg's diffraction angle (in degrees), $\beta_{1/2}$ the full-width at half-maximum (FWHM).

Ratio of HAp/ β -TCP is determined using a XRD semi-quantitative method after calibration line.

The relative intensity ratios (RIR) corresponding to the major phases observed in the XRD spectra of powders calcined at different temperatures were computed using the relationship given in eq. (4). The relative intensity ratio (RIR) of HAP to β -TCP can be calculated by the formula:

$$RIR = I_{\text{a-TCP}} / (I_{\text{a-TCP}} + I_{\text{HA}}) \quad (4)$$

using intensity peak of HA (1 2 2), and β -TCP (0 2 10).

RIR = relative intensity ratio of the phase/Sigma intensity of major line of phase/Ointensity of major lines of all phases.

The fraction of the crystalline phase of hydroxyapatite in the samples X_c was calculated using the formula:

$$X_c = 1 - \frac{V_{112/300}}{I_{300}} \quad (5)$$

where X_c is the fraction of crystalline phase, I_{300} is the intensity of (300) diffraction peak and $V_{112/300}$ is the intensity of the trough between (112) and (300) diffraction peaks.

The main characteristics of HAP powders determined from X-ray diffraction data are presented in table 2.

By analyzing data presented in table 2 it can be concluded that HAP nanopowders can be obtained by using a simple wet method of synthesis. The degree of crystallinity and the size of particles decrease by calcination. Furthermore, a mixture of nano-HAP and β -TCP has been obtained by calcination.

FTIR spectroscopy has been involved in characterization of HAP samples in order to confirm the results of X-ray

Properties	HAP-1 (dried)	HAP-2 (calcined)
Crystallite size (nm)	52.7	41.4
Content of β -TCP (%)	0	40
Degree of crystallinity (%)	88	37

Table 2
THE MAIN CHARACTERISTICS OF HAP POWDERS

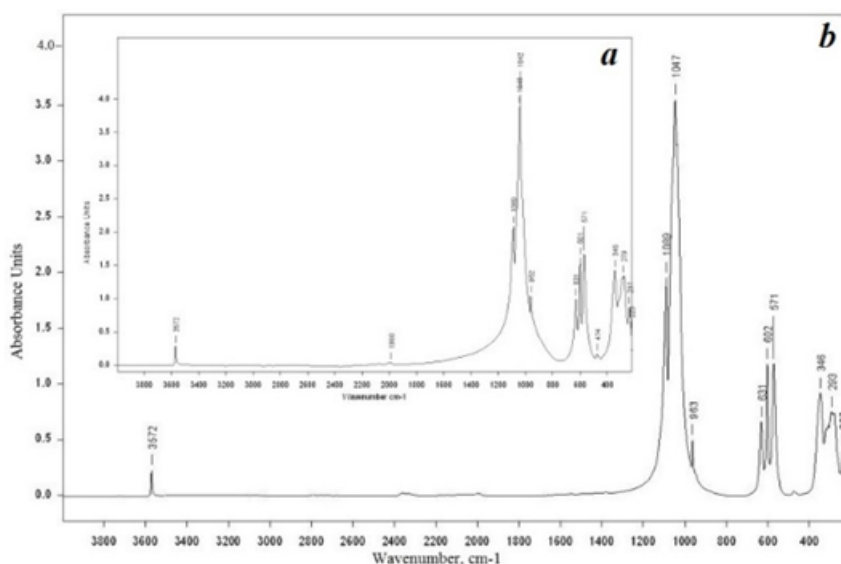


Fig. 2. IR spectra of nano-HAP samples:
a) HAP-1 (dried powder) and
b) HAP-2 (nano-HAP calcined at 900°C)

diffractograms analysis. Figure 2 depicts the IR spectra of the nano-HAP samples.

For both HAP samples, the FTIR spectrum presents only the vibration modes of phosphate and hydroxide groups in apatite structure: antisymmetric stretching mode $\nu_3\text{PO}_4$ at 1042 cm^{-1} and 1089 cm^{-1} , symmetric stretching $\nu_1\text{PO}_4$ at 962 cm^{-1} , antisymmetric $\nu_4\text{PO}_4$ and symmetric $\nu_2\text{PO}_4$ bending modes at 571-602 cm^{-1} and 474 cm^{-1} , and stretching (ν_s) and vibration (ν_l) modes of the hydroxide at 3572 cm^{-1} and 631 cm^{-1} , respectively [18, 19]. Absence of any distinct bands in the range of 1400-1550 cm^{-1} and at 875 cm^{-1} indicates that HAP does not contain carbonate ions. The carbonate formation most likely results from the interaction between atmospheric carbon dioxide and the alkaline HAP precursor solution during the synthesis process.

The specific surface area of nano-HAP samples has been estimated by the BET method. A value of 10.9 m^2/g has been determined for dried HAP sample (HAP-1), and 60.8 m^2/g for calcined nano-HAP (HAP-2).

These results show a significant decrease of particle's size and an increase of specific surface area by calcination in contrast to drying. Consequently, it is expected that a larger apatite/water interface to be accessible to heavy metals.

The sorption studies

Both nano-HAPs were investigated to the removal of Zn(II) and Pb(II) from single and binary aqueous solutions. The batch experiments have been performed in order to assess the influence of absorbent's properties and process conditions to the Zn(II) and Pb(II) removal by nano-HAP samples. Theoretical mathematically and kinetic models have been applied to experimental data in order to find the models that adequately describe the equilibrium and kinetic data related to the analyzed sorption process.

pH effect on nano-HAP sorption capacity

The first parameter analyzed was the pH because it is known from the literature that the pH of the solution

(wastewater) has an influence on the retaining of the species on the surface of the sorbent, the degree of ionization of the adsorbed molecules, the degree of dissociation of the functional groups from active adsorbent centers and ionic species of metal ions identified in real wastewater and synthetic solutions. As a result, the pH is an important parameter when it is intended to transform the sorption process from a laboratory scale to an industrial scale. The data obtained in these experiments are presented in figures 3 and 4.

As it can be seen from figures 3 and 4, the pH of the solution influences the sorption process of Zn(II) and Pb(II) on nano-HAP from single and binary solutions. At low pH values there is a competition between the protons (H^+) of the solution and Pb(II) and Zn(II) ions for active centers on the surface of the nano-HAP. Increasing the pH value decreases the number of protons in the solution and consequently the number of heavy metals ions retained by the active centers on the surface of the sorbent increases [20-22]. As a result, the amount of heavy metals ions retained per gram of nano-HAP increases to a maximum value called sorption capacity. In the case of the batch experiments performed, the pH value at which sorption capacity was recorded is 6.3 (the same value as of the pH of the initial solution of Zn(II) 100.82 mg/L). By increasing the pH above this value, there was a decrease in the amount of zinc ions retained per gram of nano-HAP, due to the fact that at high pH values in solution besides the free zinc ions there are various species of hydroxides of zinc. As a result, there is a competition between zinc elimination by precipitation as hydroxides and sorption on nano-HAP.

Similar trend has been observed for binary solution. For both heavy metals ions retained, the optimum pH value is 6. This value is the characteristic binary solution of Zn(II) and Pb(II) with 94.7 and 100.53 mg/L. Thus, further experiments in order to determine the effect of other parameters on heavy metals sorption on various nano-HAP samples will be performed at natural solution's pH.

From figures 3 and 4, it can be also concluded that a slight decrease of nano-HAP sorption's capacity has been

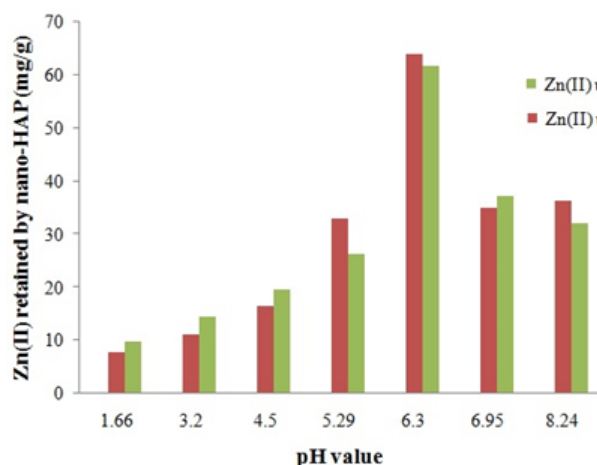


Fig. 3. The effect of solution's pH on Zn(II) retaining by nano-HAP from Zn(II) monocomponent solutions

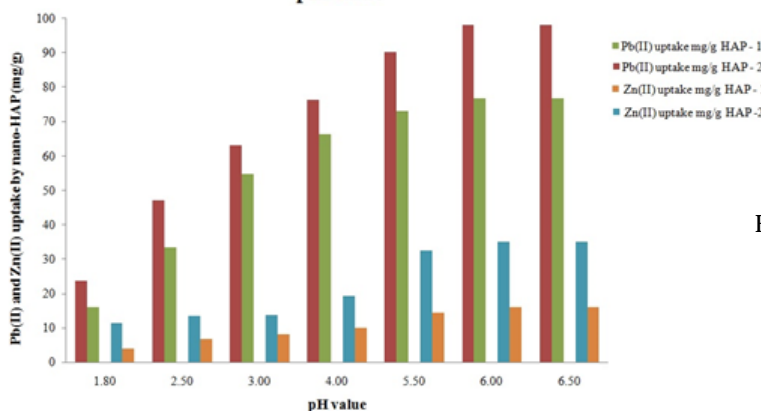


Fig. 4. The effect of solution's pH on Pb(II) and Zn(II) retaining by nano-HAP from binary solutions

registered in the process of Zn(II) removal from binary solutions compared to single solutions.

Time effect on nano-HAP sorption capacity

The second parameter we are looking for is the contact time. In order to determine the influence of the contact time on the sorption process, experiments were carried out at time ranged between 5 and 420 min. The results obtained are presented in the following figures.

Figures 5 and 6 revealed that the contact time between the two phases (the solid phase - the nano-HAP sample and the liquid - the metal ions solution) has an influence on the sorption process. In the initial phase (up to 120 minutes), the rate of the sorption process is high due to the presence of a large number of free active centers that can be occupied by the metal ions from the solution. As the contact time increases, the number of free active centers will decrease and therefore the rate of sorption process will be reduced. The contact time required to reach the equilibrium for Zn(II) sorption process on nano-HAP is 240

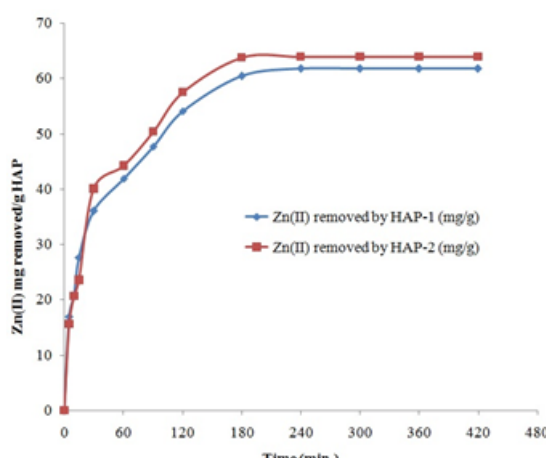


Fig. 5. Influence of contact time on the sorption process of Zn(II) on different samples of nano-HAP

min (for single solutions), and 300 min for heavy metals removal from binary solutions. These values of the optimum contact time lead to the conclusion that Zn(II) and Pb(II) sorption on nano-HAP from single and binary solution is a rapid process. The sorption capacity registered for nano-HAP has the following values: 61.75 mg Zn(II)/g for nano-HAP-1 and 63.9 mg Zn(II)/g for nano-HAP-2. The highest values of sorption capacity have been recorded for the process of Pb(II) removal from single solutions (for example: 106.84 mg/g for nano-HAP-1 and 106.91 mg/g for nano-HAP-2).

Values of sorption capacity decrease in case of binary solutions. Thus, for binary solutions the sorption capacity has the following values: 15.99 mg Zn(II)/g of HAP-1, 35.04 mg Zn(II)/g of HAP-2, 76.8 mg Pb(II)/g of HAP-1 and 98.09 mg Pb(II)/g of HAP-2. According to these values, it can be concluded that a higher decreasing of sorption capacity of Zn(II) has been registered in the presence of Pb(II) ions as competing ions for sorption centers of nano-HAP powders. In the case of Pb(II), it was recorded a slighter decreasing

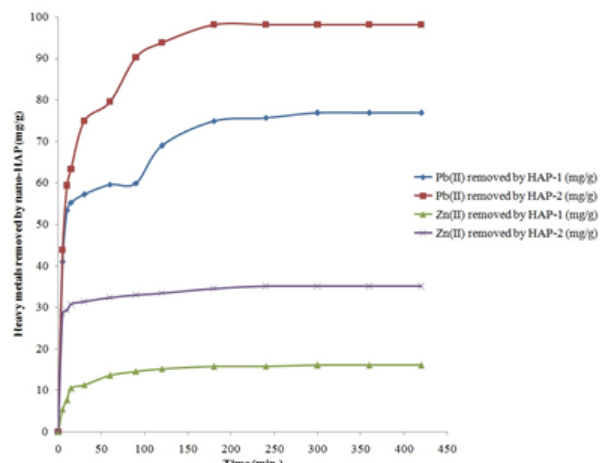


Fig. 6. Influence of contact time on the sorption process of Zn(II) and Pb(II) from binary solutions on different samples of nano-HAP

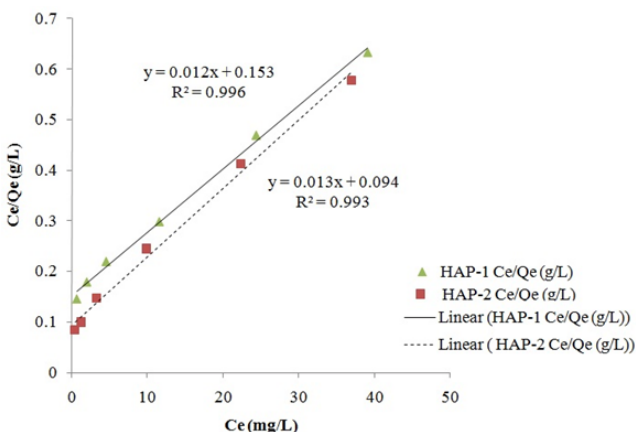


Fig. 7. Linear form of Langmuir isotherm for Zn (II) sorption on various samples of HAP

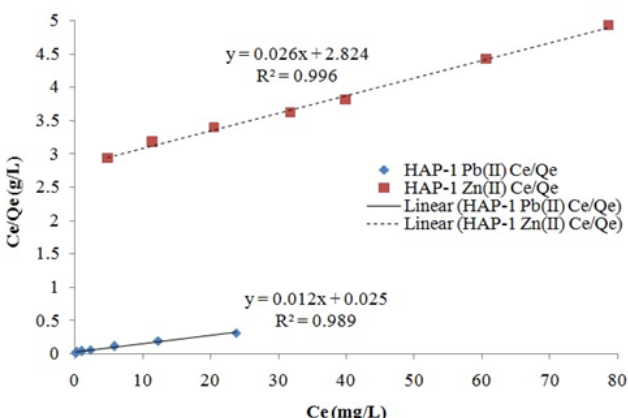


Fig. 8. Linear form of Langmuir isotherm for Zn (II) and Pb(II) sorption on HAP-1

of sorption capacity in the presence of Zn(II) ions. These results highlighted the selectivity of nano-HAP for Pb(II) ions.

Adsorption isotherms

The sorption process is mathematically characterized by the sorption isotherms. These mathematical expressions describe the relationship between the amount of dissolved substance adsorbed on the unit weight of the adsorbent and the concentration of the adsorbed in solution at a certain temperature under steady state conditions [23-25].

The Freundlich and Langmuir isotherms are most often used to characterize the sorption processes. Equation (6) is the mathematical representation of the Freundlich model, and equation (7) is characteristic of the Langmuir model [23-25]:

$$Q = K_f \cdot C_e^{1/n} \quad (6)$$

and

$$\frac{C_e}{Q_e} = \frac{1}{Q_{\max}} \cdot C_e + \frac{1}{Q_{\max} K_L} \quad (7)$$

where: K_f and $1/n$ represent the parameters of adsorption isotherms (capacity and intensity respectively); K_L is the parameter of the Langmuir model.

The Freundlich model is transformed into linear form by logarithm [23-25].

$$\ln Q = \ln K_F + \frac{1}{n} \ln C_e \quad (8)$$

For the assessment of the adsorption isotherms, experiments were carried out using the heavy metals solutions of concentrations mentioned in table 1. The experimental data obtained were processed using the Langmuir isothermal model as shown in figures 7-9.

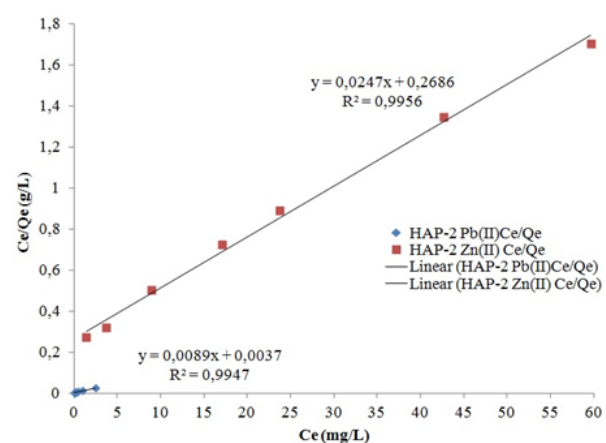


Fig. 9. Linear form of Langmuir isotherm for Zn (II) and Pb(II) sorption on HAP-2

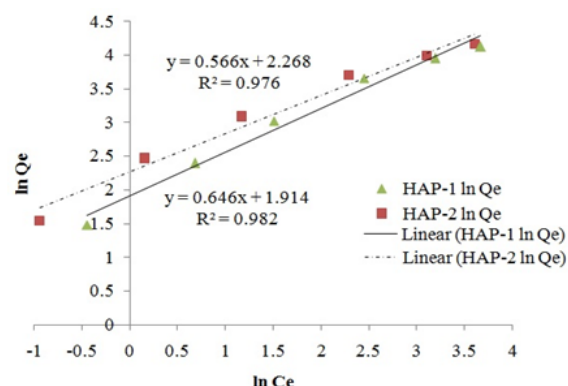


Fig. 10. Linear form of Freundlich isotherm for Zn (II) sorption on various samples of HAP

The experimental data of the Zn (II) sorption process on HAP samples were correlated with the Freundlich model. This correlation is depicted in figure 10.

For binary system, the figures 11 and 12 depict linear plots of Freundlich model for Zn(II) and Pb(II) sorption onto nano-HAP samples.

Data presented in figures 7-12 have been used to calculate the parameters of Langmuir and Freundlich isotherm models. Table 3 shows the calculated values of Langmuir and Freundlich isotherm parameters and the correlation coefficient (R^2) values for the Zn(II) and Pb(II) sorption process on HAP samples.

The data presented in table 3 shows that the Zn(II) sorption process onto HAP samples can best be described using the Langmuir isotherm (R^2 between 0.996 and 0.993).

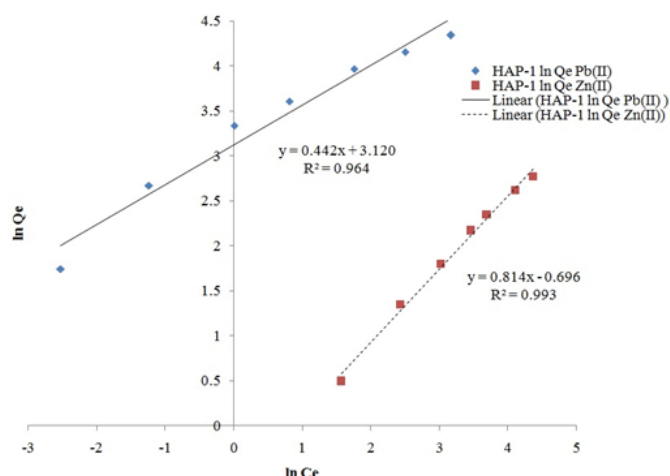


Fig. 11. Linear form of Freundlich isotherm for Zn (II) and Pb(II) sorption on HAP-1

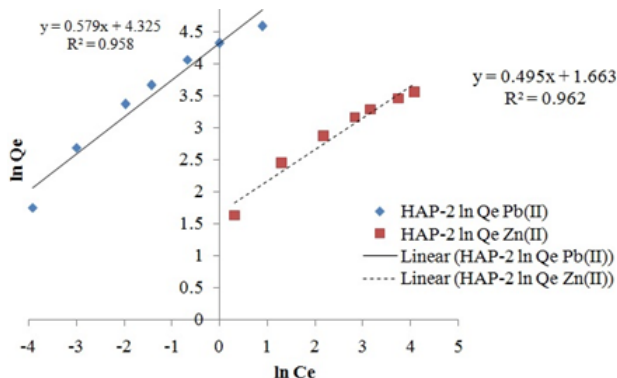


Fig. 12. Linear form of Freundlich isotherm for Zn (II) and Pb(II) sorption on HAP-2

Sorbent	Langmuir parameters			Freundlich parameters		
	Q _{max} (mg/g)	K _L (L/mg)	R ²	K _F (mg/g)	1/n	R ²
Zn(II) sorption from single solutions						
HAP-1	83.33	0.0784	0.996	6.78	0.6460	0.982
HAP-2	76.92	0.1383	0.993	9.66	0.566	0.976
Zn(II) sorption from binary solutions						
HAP-1	38.46	0.0092	0.996	0.4986	0.814	0.993
HAP-2	41.67	0.0895	0.995	4.97	0.495	0.962
Pb(II) sorption from binary solutions						
HAP-1	83.33	0.4800	0.989	22.65	0.442	0.964
HAP-2	125	2.6667	0.994	75.60	0.579	0.958

Table 3
FREUNDLICH AND
LANGMUIR PARAMETER
VALUES

According to this model, Zn(II) sorption proceeds through a monolayer sorption process on a homogeneous surface [26-30]. In addition, the experimental values of sorption capacity (61.75 mg/g, 63.9 mg/g) are close to maximum theoretical values of the sorption capacity (83.33 mg/g and 76.92 mg/g). The same conclusion can be drawn in case of Zn(II) and Pb(II) sorption onto HAP samples from binary solutions. Thus, Zn(II) and Pb(II) sorption onto nano-HAP can be described as a monolayer sorption process on a homogeneous surface.

Conclusions

The research study performed revealed that two types of HAP nanoparticles with different characteristics and sorption properties can be obtained by using a simple chemical wet method. Calcination at 900°C for 3 h leads to obtain HAP nanoparticles with lower crystallinity degree, a lower nanoparticles size and a higher specific surface than those of HAP nanoparticles dried. Furthermore, calcination has as other result obtaining of β-TCP as the secondary phase together with HAP.

Both HAP samples have been utilized in the process of Zn(II) and Pb(II) removal from single and binary aqueous solutions. The sorption capacity of HAP samples depends on the crystallinity degree, particle's size and specific surface. It has been noted that the content of β-TCP doesn't have a negative effect on sorption capacity of HAP sample. A slight higher of the sorption capacity of calcined HAP sample compared to dried HAP sample has been observed. By using single heavy metals solutions, the following values of sorption capacity have been achieved: 63.9 mg Zn(II)/g for calcined HAP, 61.75 mg Zn(II)/g for dried HAP, 106.91 mg Pb(II)/g for calcined HAP and 106.84 mg Pb(II)/g for dried HAP. These values have been decreased when the removal process have been performed with binary solutions. Thus, the values of sorption capacity are: 35.04 mg Zn(II)/g and 98.09 mg Pb(II)/g for calcined HAP, and 15.99 mg Zn(II)/g and 76.8 mg Pb(II)/g for dried HAP. It can be said that the presence of another competitor heavy metal ion has as consequence the decrease of sorption capacity. This decrease is higher in the case of Zn(II) ions

removed by dried HAP than the one registered in the case of calcined HAP. Selectivity of nano-HAP powders is higher for Pb(II) than for Zn(II).

Zn(II) and Pb(II) removal process is fast because the equilibrium has been reached after 240-300 min. The optimum value of the pH is the natural aqueous heavy metals solution. The sorption process can be described for both heavy metals tested by the use of Langmuir isotherm. Consequently, the sorption process takes place as a monolayer sorption on a homogenous surface.

The values of sorption capacity recommend using of nano-HAP powders in heavy metals removal from synthetic and real wastewater.

References

- MOHAMMAD, A.M., SALAH ELDIN, T.A., HASSAN, M.A., EL-ANADOULI, B.E., Arabian Journal of Chemistry **10**, 2017, p. 683.
- MUNEEB UR RAHMAN KHATTAK, M., ZAHOOR, M., MUHAMMAD, B., ALI KHAN, F., ULLAH, R., ABDEI-SALAM, N.M., Journal of Nanomaterials, 2017, Article ID 5670371, <https://doi.org/10.1155/2017/5670371>
- ENACHE, D.F., VASILE, E., SIMONESCU C.M., CULITA D., VASILE, E., OPREA, O., PANDELE, A.M., RAZVAN, A., DUMITRU, F., NECHIFOR, G., RSC Adv. **8**, 2018, p. 176, DOI: 10.1039/c7ra12310h
- PATESCU, R.-E., SIMONESCU, C.M., ONOSE, C., BUSUIOC, T.L., PASARICA, D.E., DELEANU C., Rev. Chim. (Bucharest), **68**, no. 1, 2017, p. 1.
- BUSUIOC, L.T., SIMONESCU, C.M., PATESCU, R.-E., ONOSE, C., Rev. Chim. (Bucharest), **67**, no. 12, 2016, p. 2504.
- TARDEI, C., SIMONESCU, C.M., ONOSE, C., SAVA, B.A., BOROICA, L., SBARCEA, B.-G., Romanian Journal of Materials **46**, no. 3, 2016, p. 289.
- KARNIB, M., KABBANI, A., HOLAIL, H., OLAMA, Z., Energy Procedia **50**, 2014, p. 113.
- TAAMNEH, Y., SHARADQAH, S., Applied Water Science **7**, 2017, p. 2021, DOI 10.1007/s13201-016-0382-7.
- SONG, M.S., VIJAYARANGAMUTHU, K., HAN, E., JEON, K.J., J Nanosci Nanotechnol. **16**, no. 5, 2016, p. 4469.
- DIXIT, A., DIXIT, S., GOSWAMI, C.S., Bioremed Biodeg 2015, 6:3.

11. EL-KAFRAWY, A.F., EL-SAEED, S.M., FARAG, R.K., EL-SAIED, H.A.-A., ABDEL-RAOUF EL-SAYED, M., Egyptian Journal of Petroleum **26**, 2017, p. 23.
12. LEI, Y., GUAN, J.-J., CHEN, W., KE, Q.-F., ZHANG, C.-Q., GUO, Y.-P., *RSC Adv.* **5**, 2015, p. 25462.
13. TARDEI, C., MOLDOVAN L., CRACIUNESCU, O., Romanian Journal of Materials, **1**, 2010, p.41.
14. PATESCU, R.-E., BUSUIOC, T.L., NECHIFOR, G., SIMONESCU, C.M., DELEANU, C., U.P.B. Sci. Bull., Series B, **79**, no. 1, 2017, p. 119.
15. PATESCU, R.-E., SIMONESCU, C.M., BUSUIOC, L.T., ONOSE, C., MELINESCU, A., Rev. Chim. (Bucharest), **67**, no. 10, 2016, p. 1899.
16. SIMONESCU C.M., PATESCU, R.-E., BUSUIOC, L.T., ONOSE, C., MELINESCU, A., LILEA, V., Rev. Chim. (Bucharest), **67**, no. 8, 2016, p. 1498.
17. VICTORIA, E.C., GNANAM, F.D., Trends Biomater. Artif. Organs **16**, 2002, p. 12.
18. METWALLY, S.S., AHMED, I.M., RIZK, H.E., Journal of Alloys and Compounds **709**, 2017, p. 438.
19. ASRI, E. EL, LAGHZIZIL, A., CORADIN, T., SAOABI, A., ALAOUI, A., M'HAMEDI, R., Colloids and Surfaces A: Physicochem. Eng. Aspects **362**, 2010, p. 33.
20. BUSUIOC, T.L., SIMONESCU C.M., PATESCU, E.-R., ONOSE, C., MELINTE, I., CAPATINA, C., POPOVICI, R.A., CRISTEA, T., Rev. Chim. (Bucharest), **66**, no.11, 2015, p. 1728.
21. SIMONESCU, C.M., TATARUS, A., TARDEI, C., PATROI, D., DRAGNE, M., CULITA, D.C., PATESCU, R.-E., BUSUIOC, L.T., **22**. SIMONESCU, C.M., MARIN, I., TARDEI, CH., DRAGNE, M., CĂPĂTINĂ C., Rev. Chim. (Bucharest), **65**, no. 7, 2014, p. 750.
23. DO, D.D., Adsorption Analysis: Equilibria and Kinetics, Imperial College Press, London, 1998.
24. CHEN, X., Information **6**, 2015, p. 14.
25. IBRAHIM, M.B., SANI, S., Open Journal of Physical Chemistry **4**, 2014, p. 139.
26. SIMONESCU, C.M., FERDES M., Polish Journal of Environmental Studies **21** no. 6, 2012, p. 1831.
27. SIMONESCU, C.M., DELEANU C., STANCU M., CAPATNA, C., Journal of Environmental Protection and Ecology **13** no. 2, 2012, p. 462.
28. SIMONESCU, C.M., DIMA, R., FERDES, M., MEGHEA, A., Rev Chim. (Bucharest), **63**, no. 2, 2012, p. 224.
29. SIMONESCU, C.M., DINCA, O.-R., OPREA, O., CAPATINA, C., Rev. Chim. (Bucharest), **62**, no. 2, 2011, p. 183.
30. DELEANU, C., SIMONESCU, C. M., CONSTANTINESCU, I., Rev. Chim. (Bucharest), **59**, no. 6, 2008, p. 639.

Manuscript received: 23.11.2018